

High sensitivity, wide coverage, and high-resolution NIR non-cryogenic spectrograph, WINERED

Yuji Ikeda^{a,b}, Naoto Kobayashi^{a,c}, Sohei Kondo^a, Shogo Otsubo^d, Satoshi Hamano^a, Hiroaki Sameshima^a, Tomohiro Yoshikawa^e, Kei Fukue^a, Kenshi Nakanishi^a, Takafumi Kawanishi^d, Tetsuya Nakaoka^d, Masaomi Kinoshita^d, Ayaka Kitano^d, Akira Asano^d, Keiichi Takenaka^d, Ayaka Watase^d, Hiroyuki Mito^f, Chikako Yasui^g, Atsushi Minami^c, Natsuko Izumi^c, Ryo Yamamoto^c, Misaki Mizumotoⁱ, Takayuki Arasaki^b, Akira Arai^b, Noriyuki Matsunaga^{a,i}, and Hideyo Kawakita^{a,d}

^aLaboratory of infrared High-resolution spectroscopy (LiH), Koyama Astronomical Observatory, Kyoto-Sangyo University, Motoyama, Kamigamo, Kita-ku, Kyoto 606-8555, Japan;

^bPhotocoding, 460-102 Iwakura-Nakamachi, Sakyo-ku, Kyoto 606-0025, Japan;

^cInstitute of Astronomy, the University of Tokyo, 2-21-1 Osawa, Mitaka, Tokyo 181-0015, Japan;

^dDepartment of Physics, Faculty of Science, Kyoto-Sangyo University, Motoyama, Kamigamo, Kita-ku, Kyoto 606-8555, Japan;

^eEdechs, 17-203 Iwakura-Minami-Osagi-cho, Sakyo-ku, Kyoto 606-0003, Japan

^fKiso Observatory, Institute of Astronomy, University of Tokyo, 10762-30 Mitake, Kiso-machi, Kiso-gun, Nagano 397-0101, Japan;

^gNational Astronomical Observatory of Japan, 2-21-1 Osawa, Mitaka, Tokyo 181-8588

^hInstitute of Space and Astronautical Science (ISAS), Japan Aerospace Exploration Agency (JAXA), 3-1-1, Yoshinodai, Chuo-ku, Sagamihara, Kanagawa, 252-5210, Japan

ⁱDepartment of Astronomy, Graduate School of Science, University of Tokyo, 7-3-1 Hongo, Bunkyo-ku, Tokyo 113-0033, Japan

ABSTRACT

Near-infrared (NIR) high-resolution spectroscopy is a fundamental observational method in astronomy. It provides significant information on the kinematics, the magnetic fields, and the chemical abundances, of astronomical objects embedded in or behind the highly extinctive clouds or at the cosmological distances. Scientific requirements have accelerated the development of the technology required for NIR high resolution spectrographs using 10 m telescopes. WINERED is a near-infrared (NIR) high-resolution spectrograph that is currently mounted on the 1.3 m Araki telescope of the Koyama Astronomical Observatory in Kyoto-Sangyo University, Japan, and has been successfully operated for three years. It covers a wide wavelength range from 0.90 to 1.35 μm (the z-, Y-, and J-bands) with a spectral resolution of $R = 28,000$ (Wide-mode) and $R = 80,000$ (Hires-Y and Hires-J modes). WINERED has three distinctive features: (i) optics with no cold stop, (ii) wide spectral coverage, and (iii) high sensitivity. The first feature, originating from the Joyce proposal, was first achieved by WINERED, with a short cutoff infrared array, cold baffles, and custom-made thermal blocking filters, and resulted in reducing the time for development, alignment, and maintenance, as well as the total cost. The second feature is realized with the spectral coverage of $\Delta\lambda/\lambda \sim 1/6$ in a single exposure. This wide coverage is realized by a combination of a decent optical design with a cross-dispersed echelle and a large format array (2k x 2k HAWAII-2RG). The Third feature, high sensitivity, is achieved via the high-throughput optics ($> 60\%$) and the very low noise of the system. The major factors affecting the high throughput are the echelle grating and the VPH cross-disperser with high diffraction efficiencies of $\sim 83\%$ and $\sim 86\%$, respectively, and the high QE of HAWAII-2RG (83% at 1.23 μm). The readout noise of the electronics and the ambient thermal background radiation at longer wavelengths could be major noise sources. The readout noise is $5.3 e^-$ for $\text{NDR} = 32$, and the ambient thermal background is significantly reduced to $\sim 0.05 e^- \text{pix}^{-1} \text{sec}^{-1}$ at 273 K. As a result, the limiting magnitudes of WINERED are estimated to be $m_J = 13.8$ mag for the 1.3 m telescope, $m_J = 16.9$ mag for the 3.6 m telescope, and $m_J = 19.2$ mag for 10 m telescope with adoptive optics, respectively. Finally, we introduce some scientific highlights provided by WINERED for both emission and absorption line objects in

the fields of stars, the interstellar medium, and the solar system.

Keywords: Infrared, Spectroscopy, High resolution, High sensitivity, Wide coverage, Non-cryogenic

1. Introduction

Near-infrared (NIR) high-resolution spectroscopy is an essential observational method in astronomy. It enables us to improve the detectability of the weak and narrow lines of the objects brightened in the infrared region, such as the cool stars, the embedded and/or hidden stars in the circumstellar and the interstellar mediums, and cosmologically distant QSOs. It also provides additional significant information concerning the kinematics and the magnetic fields of astronomical objects with the Doppler broadening and the shift due to the Zeeman effect. Doppler searches of exoplanets revolving around M-type stars and YSOs are one of the most prevalent uses of infrared high-resolution spectroscopy^[1-4]. For the Zeeman effect, because the Zeeman shift, $\Delta\lambda/\lambda$, is proportional to λ , it is easily detectable in the infrared region. In addition, NIR high-resolution spectroscopy enables us to resolve atomic and molecular lines, which cannot be detected in the other wavelength regions. Absorption lines of rare metals like s-process elements in the stellar spectra and rotational structures of electronic/vibrational bands of molecules yield the temperature and the density of interstellar and circumstellar gas and the isotope abundances, which are closely related to the nucleosynthetic and chemical processes in the universe. In addition, we can observe the non-polar molecules, such as H₂, CH₄, and CO₂, with their electric quadrupole transitions, which are not detectable in the radio region. Technically, high resolution spectroscopy provides an advantage with regards to the data quality because it can isolate the lines of interest the telluric emission and absorption lines, which often bother astronomers in this wavelength region. The applications of the infrared high-resolution spectroscopy include multiple scientific fields and are rapidly expanding with the development of new technologies (e.g., Käufel et al. 2005)^[5].

NIR high-resolution spectroscopy ($R > 20,000$) was initiated with the technological innovation of infrared arrays in the early 1990's. It was first used by CGS4^[6] on UKIRT and CSHELL^[7] on IRTF, which employed 256 x 256 InSb arrays. In the 2000's, cross-dispersed type high-resolution spectrographs were developed for 10 m telescopes using 1k x 1k format IR arrays, NIRSPEC^[8] for Keck2 and IRCS^[9] for Subaru, even though their spectral resolutions were still $R = 25,000$ and $R = 20,000$, respectively. In 2007, a new cross-dispersed type spectrograph, CRIRES, was commissioned for the VLT with a maximum spectral resolution of $R = 100,000$ ^[10,11], and became to be recognized as a new but routine scientific tool, especially in the fields of stars and interstellar medium. After 2010, NIR high-resolution spectrometers with widely differing purposes were developed with large 2k x 2k format infrared arrays and new technologies, such as IR fiber and immersion grating. The APOGEE spectrograph^[12,13] on the 2.5 m telescope at the Apache Point Observatory is a multi-object high-resolution spectrograph in the H-band with $R=22,500$. Its aim is the spectroscopic survey of 100,000 stars in the Milky Way, which started from 2012. GIANO^[14,15] on TNG and IGRINS^[16] on the 2.7 m telescope of the McDonald Observatory aim to achieve a wide spectral coverage in the J-, H-, and K-bands with $R = 50,000$ and in the H- and K-bands with $R = 45,000$. IGRINS employs a Si immersion grating developed by a group at the University of Texas^[17,18]. At present, a few new spectrographs with much higher resolution spectrometers are under development and will be commissioned soon, e.g., iSHELL^[19] on IRTF ($R = 70,000$ with Si immersion gratings), IRD^[20] on Subaru ($R = 70,000$), and CRIRES+^[21] on VLT ($R = 100,000$).

Under these conditions, we have been developing a new NIR high-resolution spectrograph called WINERED^[22-24]. In 2013, it was commissioned on the 1.3 m Araki telescope at the Koyama Astronomical Observatory of Kyoto-Sangyo University in Japan. WINERED is a PI-type instrument that can be attached to various telescopes with a Nasmyth focus (Figure.1). It covers a wide wavelength range from 0.90 to 1.35 μm (z-, Y-, and J-bands) with $R = 28,000$ and $R = 80,000$ (see Table.1). The main goal of WINERED is to obtain high-resolution infrared spectra with high signal-to-noise ratios (SNR) and high-quality, which has been achieved with the state-of-the-art optical echelle spectrographs in the optical region. To achieve this goal, WINERED has three distinctive features: (i) optics with no cold stop, (ii) wide spectral coverage, and (iii) high sensitivity. The first feature reduces the time for development, alignment, and maintenance, as well as the total cost. WINERED has become a prototype for a high resolution spectrograph for 30 m telescopes, because it is technically difficult to build an extremely large cryogenic instrument. The second feature, wide coverage, is an adapted concept for GIANO and IGRINS, which are capable of obtaining accurate physical parameters such as the temperature, the density, and the chemical abundances, because WIERED enables simultaneous measurements of several atomic lines or the entire

electron/vibrational-rotational structures for molecular lines. The third feature, high sensitivity, is the greatest feature of WINERED. This is achieved with WINERED’s unprecedentedly high throughput optics (Section 2), the low noise system (Section 3), and the extremely reduced thermal background (Section 4.2). In this paper, we briefly describe the instrumental designs and performances of WINERED’s Wide-mode. In addition, we introduce scientific highlights obtained by WINERED and our future plans. See Otsubo et al.^[25] for the details concerning the Hires modes with $R = 80,000$.

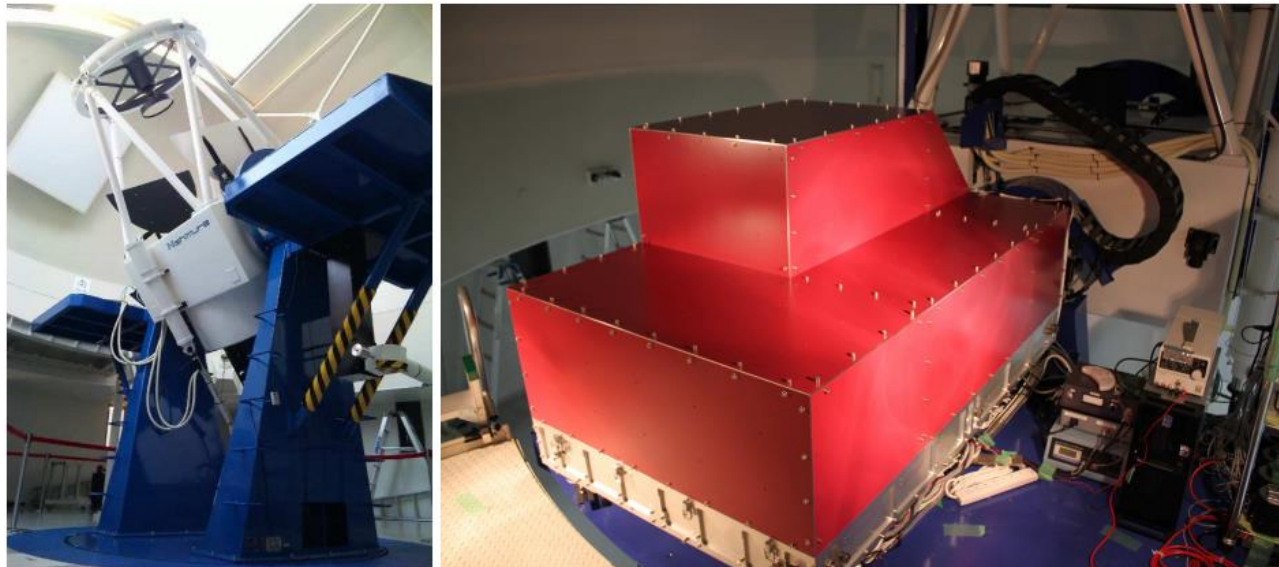


Figure 1. The 1.3 m Araki telescope (left) and WINERED (right).

Table 1. Summary of WINERED’s specifications.

		Wide mode	Hires-Y mode	Hires-J mode
Telescope	Diameter f/#		Any f/11	
Overall	Wavelength coverage	0.90 - 1.35 μm	0.96 - 1.11 μm	1.14 - 1.35 μm
	Nominal spectral resolution	28,000	80,000	80,000
	Slit width		100 μm , 200 μm , and 400 μm	
	Slit length		3.12 mm	
	Optical magnification factor		0.346	
	Total throughput	> 50%		> 35 %
	Instrumental volume	1750 mm (L) x 1070 mm (W) x 500 mm (H)		
	Operation temperature	270 - 300K (for optics except for the camera lens and the detector)		
Detector	Format	2048 x 2048 pixels (HAWAII-2RG 1.7 μm -cutoff)		
	Pixel size	18 μm x 18 μm		

2. Optics

Figure 2 shows the optical layout of WINERED. WINERED’s main optics of WINERED consists of six optical elements, “the slit stocker”, “the collimator lens unit”, “the main dispersers”, “the cross-dispersers”, “the camera lens unit”, and “the infrared array”. All optical elements, except for the camera optics and the infrared array, are maintained at the room temperature, as are optical spectrographs. WINERED does not employ “white-pupil type optics”, which is often adapted for modern large spectrographs, to maximize the total throughput with the minimum number of optical surfaces (The white-pupil type optics requires an additional optical surfaces, such as a relay optics for making a second pupil on the main disperser or the cross-disperser).

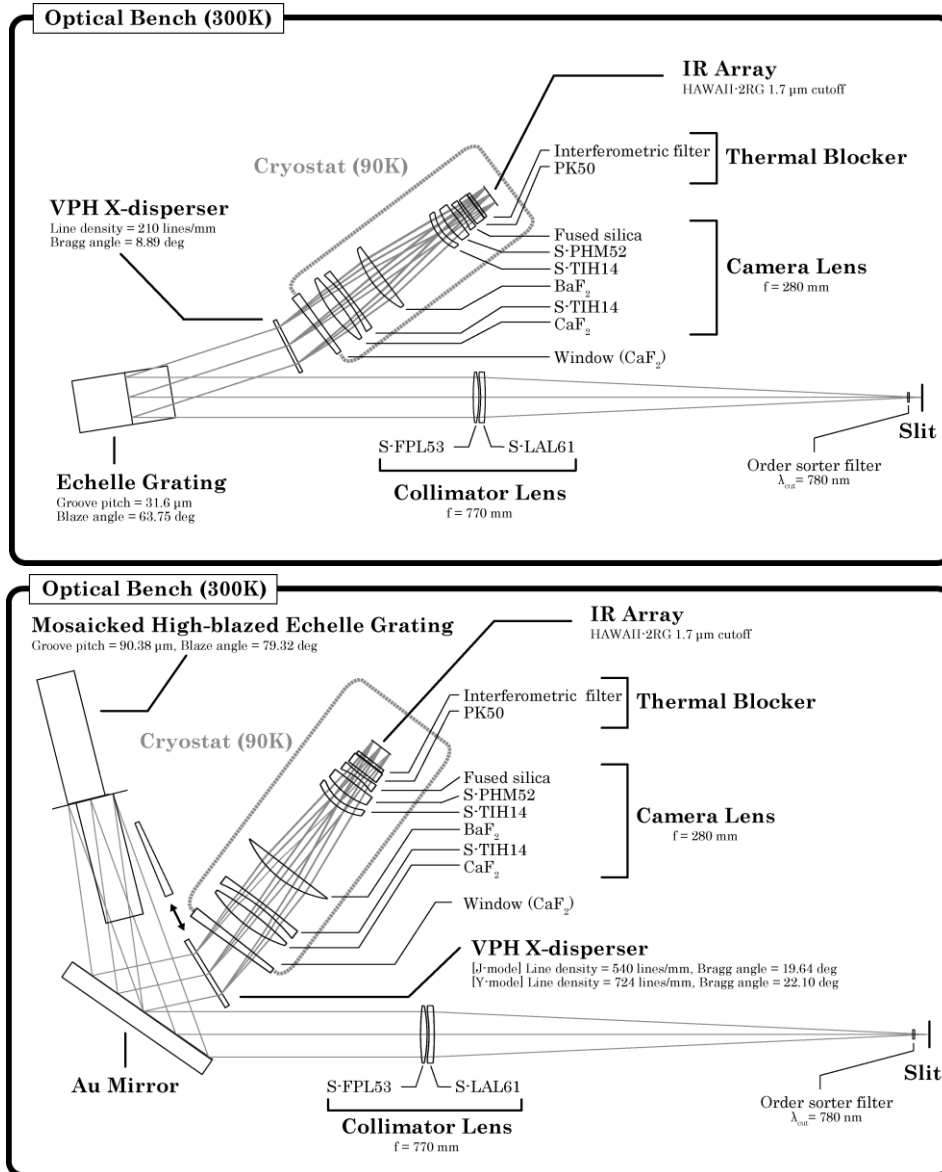


Figure 2. Optical layout of WIDE-mode (top) and Hires-Y and J modes (bottom) of WINERED. The optical elements are located on the optical bench with the room temperature, except for the camera lens and infrared array that are installed under the cryogenic condition with $T = 90 \text{ K}$ and 77 K , respectively. See text for more details.

The slit stocker has three types of slits with different slit widths (100 μm , 200 μm , and 400 μm) and a pinhole used for the verification and alignment of the instrument. Each slit provides a different spectral resolution of 28,000, 14,000, and 7,000 for the Wide mode and 80,000, 40,000, and 20,000 for the Hires-Y and Hires-J modes, respectively. The slits are formed on the aluminized mirrors and are tilted by 20 degrees from the telescope optical axis. The reflected focal plane images from the slits are reflected to the slit viewer system using the re-imaging optics with a magnification factor of 0.295. A commercially-available CCD camera is used for the slit viewer. An order-sorter filter is just inserted after the slits' stocker to reduce the second-order light between 0.45 μm and 0.78 μm produced by the following cross-dispersers. The transmittance is $> 98 \%$ at 0.9 – 1.35 μm (in the WINERED wavelength region) and $< 1 \%$ at less than 0.7 μm . The stellar light, which passed through this order-sorter filter, is collimated using the collimator lens unit with an effective focal length of 770 mm. The collimator lens unit consists of two glass spherical lenses, S-FPL53 and S-LAL61. The total transmittance

of the collimator lens unit is > 98 % due to the high quality BBAR ($R < 0.5$ % for in the WINERED wavelength region). A collimated beam with a diameter of 70 mm is dispersed via the echelle gratings, which act as the main disperser. WINERED employs two echelle gratings, a classical echelle grating for the Wide mode and a high-blazed echelle grating for the Hires-Y and J modes. The classical echelle grating is fabricated by Newport Inc., US. It has a blaze angle of 63.75 degrees and a groove pitch of 31.6 μm . The maximum absolute diffraction efficiency reaches 83 %^[23]. The high-blazed echelle grating is custom-made by Canon Inc., Japan. It has a blaze angle of 79.32 degrees, a groove pitch of 90.32 μm , and an apex angle of 88 degree. The absolute diffraction efficiency is 68 % even with a high blaze angle (see Otsubo et al.^[25] for more details concerning the high-blaze echelle grating and the Hires modes). The dispersed light from the echelle gratings is divided into each order using the cross-dispersers. Different VPH gratings are prepared as the cross-dispersers of each mode. While the Wide mode VPH shows a lower dispersion with a Bragg angle of 8.9 degrees and the a density of 270.0 lines mm^{-1} , the Hires-Y and J mode VPHs show higher dispersions with the Bragg angles of 22.1 degrees and 19.65 degree, and the line densities of 720.80 lines mm^{-1} and 540.48 lines mm^{-1} , respectively. A prism with an apex angle of 8.1 degree is glued to the exit surface of the Hires-Y VPH grating to reconcile the direction of the exiting beam with that of the Hires-J mode. All the VPH gratings were fabricated by Wasatch photonics, US. The maximum diffraction efficiencies are 86 % for the Wide mode, and 91 % for both Hires-modes. The dispersed light is focused by the camera lens unit and forms an echellogram on the infrared array (see Figure 3). The focal length and the clear aperture are 266.8 mm and 128 mm, respectively. The camera lens unit consists of six spherical lenses, CaF_2 , S-TiH14, BaF_2 , S-TiH14, S-PHM52, S-FPL51, and fused silica. It is operated at 90 K in the cryostat. The dielectric multi-layer films are coated on the fused silica lens, which plays a role as the thermal blocker from the ambient thermal background radiation, in cooperation with two filters (a PK50 filter and an H-band cut filter) installed between the camera lens and the infrared array (see section 4.2). The total transmittance of the camera lens unit and the thermal blocker filter are achieved to be 91 % and 95 %, respectively. WINERED uses HAWAII-2RG 1.7 μm cutoff array as its detector. It is sufficient to achieve WINERED's concept of "high sensitivity" because it is currently the most sensitive infrared array for astronomical applications owing to its high QE and low readout noise. In actuality, the QEs of HAWAII-2RG used in WINERED have been measured at 72 % in 0.8 μm , 63 % in 1.0 μm , and 87 % in 1.23 μm (see also Table 2). Figure 3 shows the echellograms of a planetary nebula NGC7027 and the flat-fields spectrum in Wide mode. The entire wavelengths from 0.9 μm to 1.35 μm is continuously (no-disconnectedly) collected in the infrared array with good image quality.

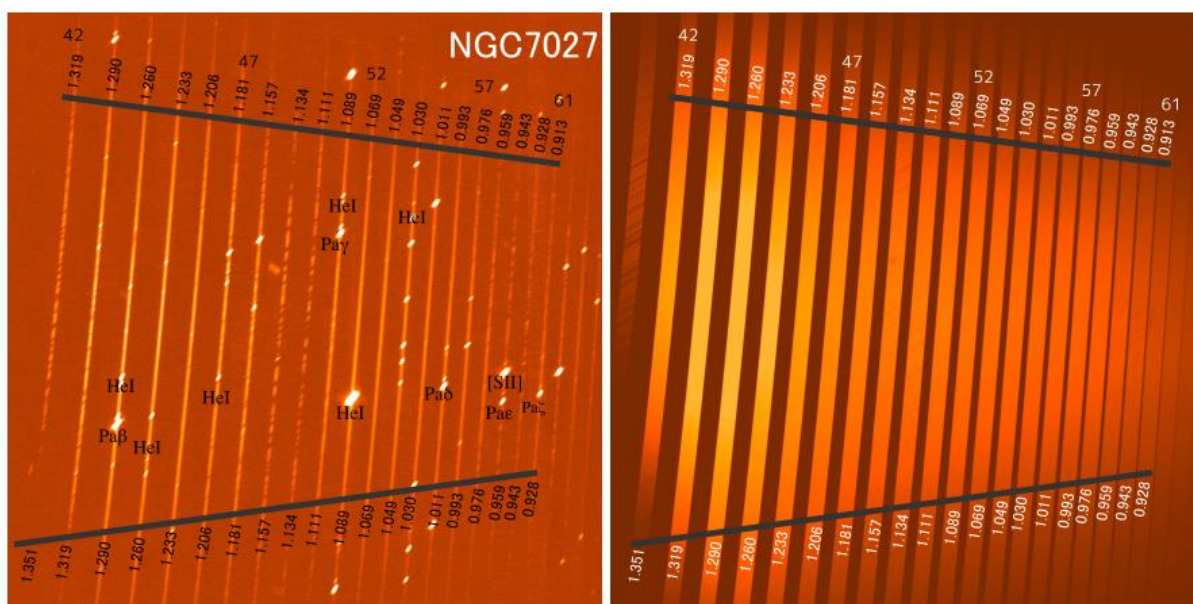


Figure 3. Echellograms in the Wide mode: NGC7027 (left) and a flat-lamp (right). The area between the two black lines show the free spectral range, and numbers indicate the shortest and longest wavelengths in μm for each order.

3. Detector

WINERED employs a HAWAII-2RG 1.7 μm -cutoff array provided by Teledyne Inc., US. It achieves a high QE and no fringe via the removal process of the thin CdZnTe substrate covering the HgCdTe array (which detects infrared wavelengths). In addition, with the reference pixels arranged along the frame of the array, the read noise is dramatically reduced^[26, 27]. For the readout and the control of the array, we use a SIDECAR ASIC and the JADE2, which are also provided by Teledyne Inc. SIDECAR ASIC is installed into the cryostat with an operation temperature of approximately 80 K, and the JADE2 is attached on the outer wall of the cryostat at room temperature. The SIDECAR ASIC and the JADE2 are directly connected with a custom-made flat cable with 80 pins and a length of 350 mm. A rectangle hole is cut into the outer wall of the cryostat through which this cable is run. The gap between the wall and the cable is sealed using the epoxy adhesive STYCAST on which another epoxy adhesive 631-C (Aremco Products, Inc.) is over-coated.

WINERED usually operates in 32-ch mode with a readout speed of 100 kHz for the readout. To reduce the effect of the latency (see below), four time resets are provided before every exposure; therefore, it always takes $(t_{\text{exp}} + 14)$ for an exposure with t_{exp} . The evaluation results of the array system for WINERED are summarized in Table 2. The QEs are measured by Teledyne Inc., using infrared LEDs, at 120 K. The values are slightly scattered depending on the wavelength. The dark current was measured to be $7.63 \pm 0.2 \times 10^{-3} \text{ e}^- \text{ sec}^{-1}$ at 80 K and it is negligible for normal observations. Figure 4 shows the measurement results of the read noise depending on NDR. We find that NDR gradually decreases in good agreement with the expected curve, which is $\propto \text{NDR}^{-1/2}$. The well capacity (full well) is approximately 13,700 e^- , which is defined as the maximum number of electron for fulfilling the 5 % linearity.

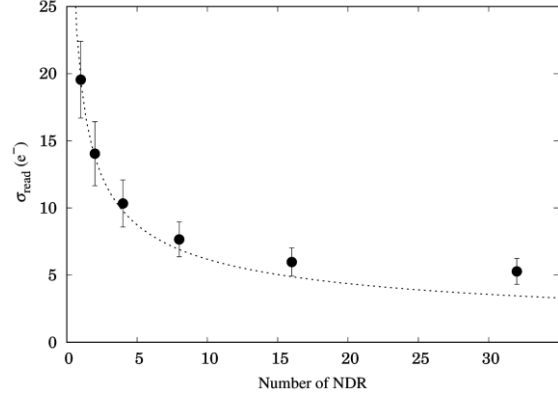


Figure 4. Measurement results of the read noise.

WINERED's HAWAII-2RG has a somewhat large latency. The latency drops by 0.14 % after two resets as reported by Teledyne Inc.; however, the remaining electrons do not clear up for greater than one hour. The effect on the spectra is sufficiently small for general observations because it is nearly canceled by the subtraction of sly frames taken after the exposure (the changing rate of the counts by the remaining electrons is very slow). However, we need to be careful in observations including emission line objects, such as planetary nebula and/or faint objects for which strong airglow emission lines are printed in the frames. We plan to develop a reduction method to correct the latency effect, even for these objects.

Table 2. Specification and evaluation results of the array electronics system for WINERED

	Specifications	Measured performances	Remarks
Material	HgCdTe	-	
Pixel format	2048 pixel x 2048 pixel	-	
Pixel size	18 μm	-	
Cutoff wavelength	1.65 - 1.80 μm @ 120K	1.70 - 1.75 μm @ 120 K	By Teledyn Inc.
QE	> 50 % @ 0.8 μm > 50 % @ 1.0 μm	72 % @ 0.8 μm 63 % @ 1.0 μm	By Teledyn Inc., measured at 120 K
Dark current	> 70 % @ 1.23 μm < 0.05 e^-/sec @ 120 K	87 % @ 1.23 μm $7.63 \pm 0.2 \times 10^{-3} \text{ e}^-/\text{sec}$ @ 80 K	For $V_{\text{bias}} = 0.25 \text{ V}$
Read noise	< 30 e^-	$19.2 \pm 2.9 \text{ e}^-$ for NDR = 1 $5.3 \pm 1.0 \text{ e}^-$ for NDR = 32	
Well Capacity	> 80,000 e^-	13,700 e^-	For $V_{\text{bias}} = 0.25 \text{ V}$, defined as the range of the linearity of < 5 %

4 Performances

4.1 Spectral resolution

Figure 5 shows the spectral resolution measured for the Wide-mode. Here, the spectral resolution is defined as the FWHM of the monochromatic slit image for each wavelength. We used a one-dimensional spectrum obtained from the integration of one hundred ThAr lamp images for wavelength calibration, which were reduced with a standard reduction software for WINERED^[28]. The solid lines in Figure 5 are the simulated spectral resolution from the first-order ray tracing (not considering any aberrations), which agree with measured spectral resolutions in the entire of WINERED wavelength region.

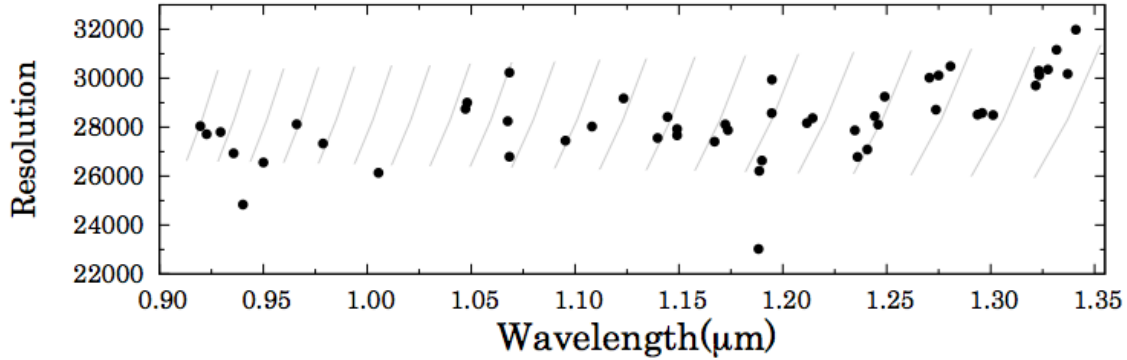


Figure 5. Measured spectral resolution in Wide mode. The solid lines are simulated spectral resolution from the optical design.

4.2 Non-cryogenic performance

Because WINERED has no cold stop, the ambient thermal background radiation through the camera lens system directly reaches the infrared array (see Figure 2). Several non-cryogenic infrared instruments have been proposed and examined since Joyce et al.^[29]; however, no one has yet succeeded as far as we know^[30,31]. Amado et al.^[31] presented three solutions to achieve non-cryogenic infrared instruments:

- Using an infrared array possibly with a short cutoff wavelength;
- Reducing the solid angle seen from the infrared array using cold baffles that are as small as possible; and
- Employing a filter blocking the penetration of the thermal background radiation.

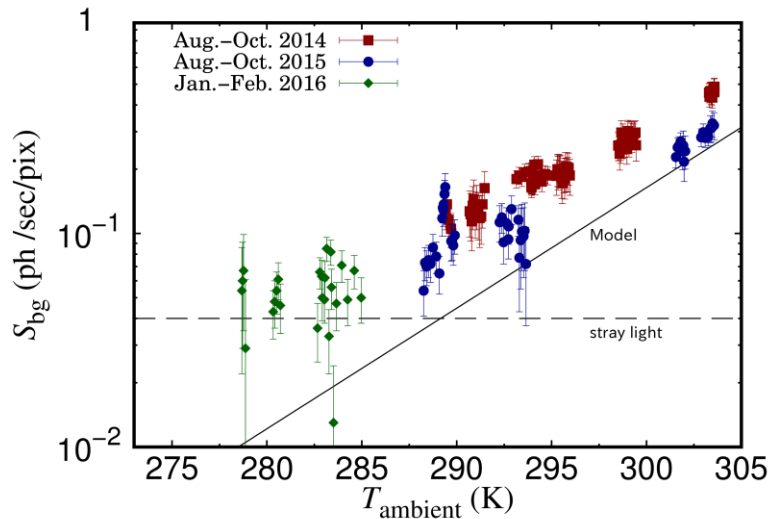


Figure 6. The measured thermal background radiation reaching the array at various the ambient temperatures. The difference in the plots reflects the different seasons. The solid line is the predicted flux assuming that the ambient environment is a black body. The dashed lines are the levels of stray light in the cryostat, which were evaluated using the other experiments.

WINERED adapts all three solutions to build a non-cryogenic high-resolution spectrograph with a comparable or greater sensitivity compared to classic cooled spectrographs. First, we employ the HAWAII-2RG 1.7 μm -cutoff array. It provides the highest QE of the available infrared arrays with a short cutoff wavelength, less than 2.0 μm at present. Second, we place the camera lenses in an entirely enveloped tube-barrel, which plays the role of a cold baffle in the cryostat. As a result, only the f/2 conical radiation enters the array at the center of the array in the design. Finally, there thermal blocker filters are installed between the camera lens system and the infrared array. The first filter is an interference multi-layer filter coated on both surfaces of the last (6th) lens, which reflects back the radiation in the H- and K-bands; the second filter is a glass filter made of PK50, which absorbs the radiation greater than 2.5 μm ; and the third filter is an interference filter, which dramatically reduces the radiation in the H-band region. Figure 6 shows the total fluxes of the ambient thermal background radiation detected by the WINERED array. These are estimated from several frames with long time exposures of > 300 sec at night in each season. It can be confirmed that the ambient thermal background radiation is successfully suppressed below 0.1 photons $\text{pix}^{-1} \text{sec}^{-1}$ at 290 K (the target values are 0.1 photons $\text{pix}^{-1} \text{sec}^{-1}$ at 290 K and 0.03 photons $\text{pix}^{-1} \text{sec}^{-1}$ at 273 K). The plots at temperatures greater than 290 K agree with the solid line representing the predicted fluxes from a perfect black body. The deviation in the plots from the solid line near 280 K is attributed to stray light originating from a slit structure cut in the array cassette. This component is approximately 0.04 photons $\text{pix}^{-1} \text{sec}^{-1}$ (plotted as the dashed line in Figure 6). This stray light is negligible for normal observations, except for faint objects, because it slightly changes the limiting magnitude by $\Delta m_J \sim 0.4$ at 273 K and $\Delta m_J \sim 0.2$ at 290 K.

4.3 Throughput and limiting magnitude

Figure 7 shows the total throughput for WINERED’s Wide mode, which is measured using a spectroscopic standard star HD51956 (F81b) with a 400 μm slit (i.e., 6 arcsec for the 1.3m Araki telescope). Because the seeing size was 3 - 4 arcsec on that night, nearly all the photons entered the slit. The total exposure time was 300 sec. The transmittances of the Earth’s atmosphere, the telescope throughput, and the array QE, which need to be assumed for the correction, are given by the grey, dashed, and dotted lines, respectively. The transmittance of the atmosphere was predicted by LBLRTM^[32,33]. The relative humidity was assumed to be 70 % (which is a typical value for Kyoto) and the same zenith distance was used as the observed star for the calculation. The telescope throughput includes the reflectivities of the primary, the secondary, and tertiary mirrors, and the obstruction by the secondary mirror (0.94). The reflectivities of the mirrors were obtained via measurements at 1.064 μm . The array’s QE was linearly interpolated from the measurement results in Table 2. The final throughputs of WINERED’s Wide mode were $\sim 30\%$ in the z-band, $> 40\%$ in the Y-band, and $> 50\%$ in the J-band.

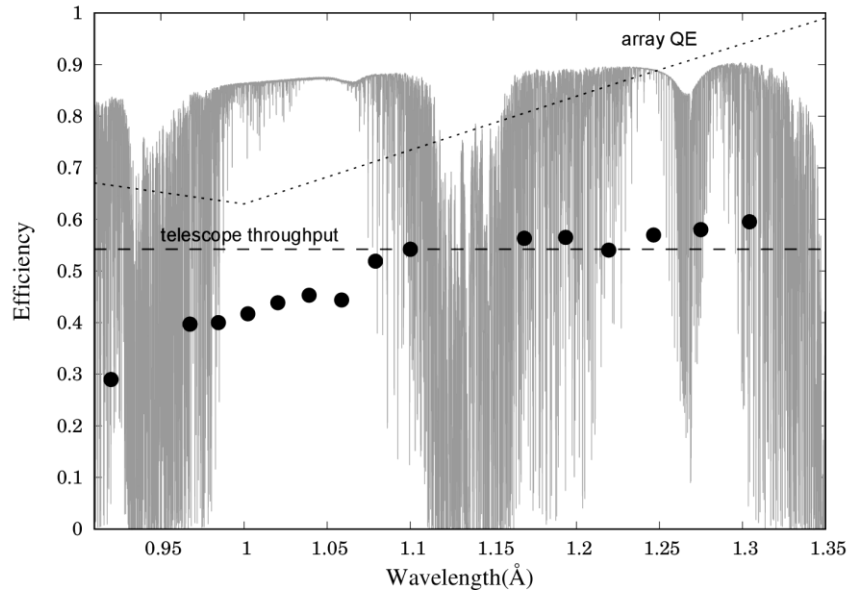


Figure 7. The total throughput of WINERED’s Wide-mode (full circles), not including the slit loss. The grey, dashed, and dotted lines are the theoretical atmospheric transmittance by LBLRTM, the telescope throughput assumed from the measurement at 1.063 μm , and the quantum efficiency interpolated from the measurements, respectively. See the text for more details.

Surprisingly, these values are much higher than those of the other infrared high resolution spectrometers (e.g., at most 15 % for NIRSPEC, IRCS, and CRIRES^[8-11]), even though they would be compared with the optical spectrographs. Table 3 shows the calculated limiting magnitudes in the J-band for various telescopes with different diameters. The array noise (the readout noise and the dark noise) from Table 2, the background radiation and the stray lights from Figure 6, and the total throughput from Figure 7 are considered. The limiting magnitude is defined as the magnitude at which a spectrum with SNR = 30 can be obtained with the total exposure time of 8 hours. The limiting magnitude of 19.2 mag for a 10 m telescope has never achieved with previous or currently planned instruments. This limiting magnitude was first realized due to WINERED's peerlessly high throughput and low noise performance.

Table 3. The estimated limiting magnitudes in the J-band for various telescopes (for SNR = 30 and a total exposure of 8 hrs).

Telescope	Araki	NTT	Keck
Observatory	KAO	La Silla	Mauna Kea
Location	Kyoto, Japan	Atacama desert, Chile	Hawaii, US
Diameter	1.3 m	3.6 m	10.0 m
Slit width	1.5''	0.49''	0.19''
Assumed seeing	3.0''	0.8''	0.2'' w/ AO
Limiting magnitude (m)	13.8	16.9	19.2

5. Scientific highlights

Here, we introduce few of the scientific results obtained using the Wide mode ($R = 28,000$) of WINERED since it was commissioned in 2013. Figure 8 shows the spectrum of a late type star, ϵ Leo (G1II), which is also a metal standard star whose chemical abundances have been well-investigated to be used for calibration purposes when measuring the abundances of various stars. We had previously developed a high accurate method to correct telluric absorption lines^[34], which often inconvenience astronomers dealing with infrared spectra. Due to the accurate corrections provided by this method, we can detect many faint lines, even to less than a few %, of which some parts had not been detected in the previous observations. In addition, large differences in the strengths are observed between the observed and synthetic lines for several lines. This is due to the use of incorrect physical parameters, such as oscillator strengths ($\log g_f$), when producing the synthetic spectrum. Therefore, we can update and correct these physical parameters corrected with this spectrum. We will release new line catalogs in the WINERED wavelength region for various types of stars, including newly detected metal lines and more accurately calibrated $\log g_f$.

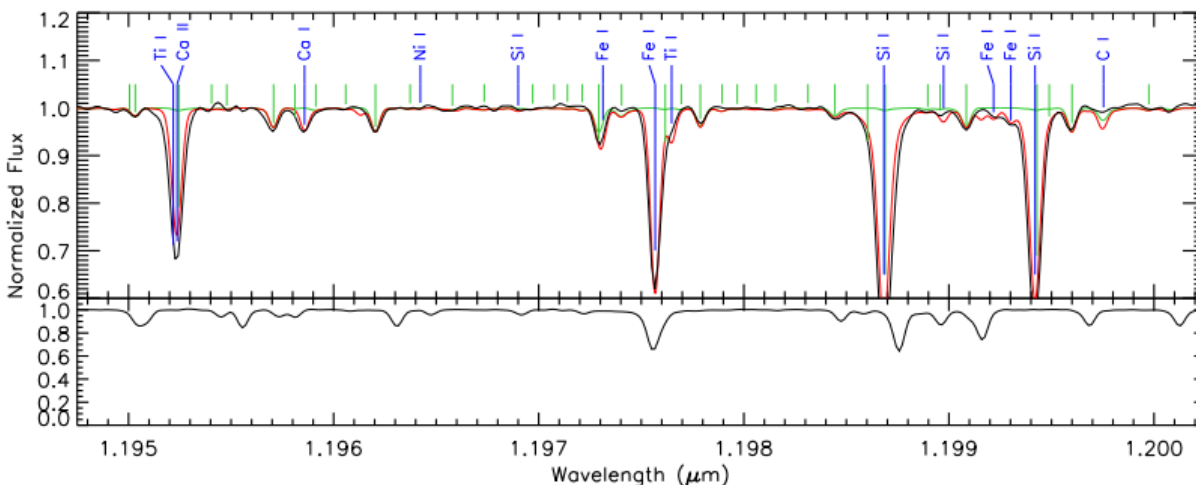


Figure 8. The J-band spectrum of ϵ Leo (the black line in the upper panel). The red line is a synthetic spectrum with stellar parameters obtained from the high resolution spectra in the optical region. The green bars show the CN absorption lines. The bottom panel is the spectrum of an A0V star in which the absorption lines indicate the telluric lines.

Figure 9 shows extremely high quality spectra (with the SNRs of ~ 700 for the Y-band and ~ 500 for the J-band) of a bright B star embedded in the high mass star-forming region, Cyg OB2 No.12. For comparison, the spectra of β Ori (B8Ia) are also shown in the upper panel. The spectra should not have absorption features from the interstellar medium because of $E_{B-V} = 0$. We can find several absorption lines (indicated by the vertical red bars) that cannot be seen in the β Ori's spectra. These are the newly detected diffuse interstellar bands (DIBs) found by WINERED, except for the strongest one, DIB10780, which had previously been detected by Groh et al.^[35]. WINERED has already discovered approximately 50 weak DIBs in the near infrared region using these high SNR spectra^[36-38].

Finally, we show an example of an emission line object, a comet C/2013 R1 (Lovejoy), in Figure 10. In the Y-band, there are strong lines of the electronic transition of the CN red system, which had not been well investigated with high-resolution spectroscopy because of a niche wavelength region that was insensitive to both CCDs and IR arrays. The population distribution of CN among the rotational energy levels indicates the physico-chemical conditions of the cometary coma^[39].

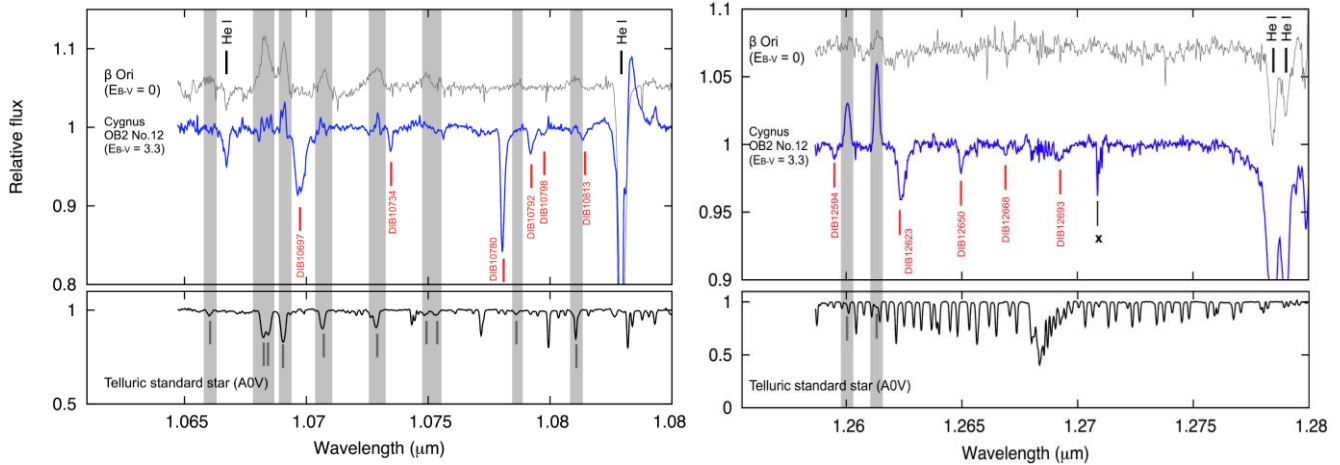


Figure 9. The top panels show the Y-band (left) and the J-band spectra of Cyg OB2 No.12 (right), together with the spectra of a reference star, β Ori, which are drawn with grey lines. The newly detected weak DIBs are indicated with red vertical bars; only the strong line DIB10780 had previously been detected. The bottom panels show the spectra of a telluric standard star (A0V), which were used to correct the telluric absorption lines (however, there are many weak metal absorption lines in A0V type stars in this region that are masked by the gray shaded areas).

6. Summary

We developed a new NIR high-resolution called spectrograph WINERED. Our goal is to achieve wide coverage and high sensitivity with $R = 28,000$ (Wide mode) and $R = 80,000$ (Hires-modes) using a non-cold stop optics. Owing to a state-of-art optical design and a high performance infrared array, we achieved a total high throughput ($> 50\%$) and an ideal reduction of ambient thermal background radiation of less than $0.05 \text{ photons pix}^{-1} \text{ sec}^{-1}$ for the Wide-mode (which covers the entire z-, Y-, and J-bands in a single exposure). WINERED has the potential to reach deeply embedded objects in the circumstellar and interstellar mediums, supergiants and giants in the nearby galaxy, and the distant galaxies with high redshifts with its overwhelming limiting magnitudes of $m_J > 17 \text{ mag}$ for 4m-class telescopes and $m_J > 19 \text{ mag}$ for 10m-class telescopes.

We will complete the remaining Hires-modes using a high efficiency high-blazed echelle grating (R5.3) by the summer of 2016. It has been confirmed that the Hires-modes provide the expected performances for the spectral resolution and sensitivity.^[25] The combination of the Wide- and Hires- modes should widen the scope of WINERED's activities in various fields of astronomy.

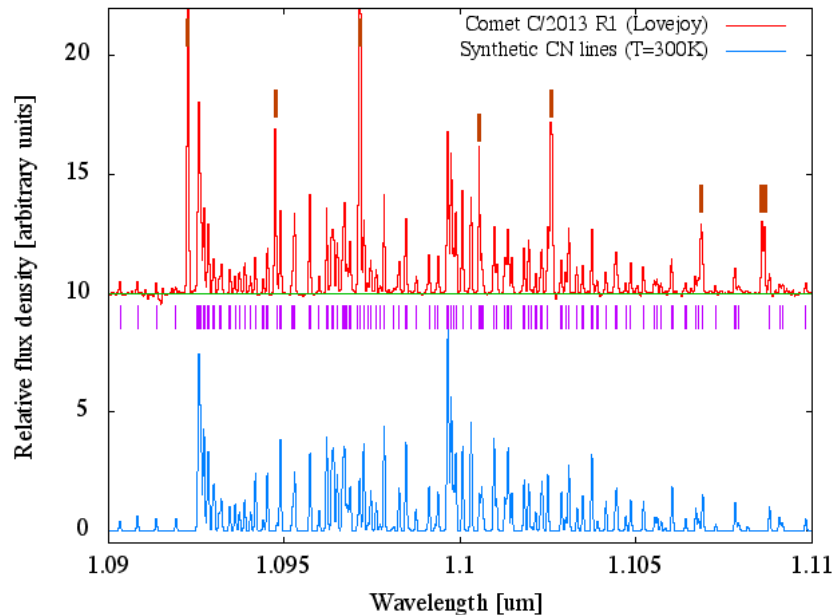


Figure 10. The emission band of the CN red system in comet C/2013 R1 (Lovejoy). The upper spectrum is the observed cometary emission spectrum (in which the reflected solar spectrum from the cometary grains has been subtracted). The lower spectrum is the synthetic CN spectrum, indicated with purple vertical bars for each ro-vibronic transition of CN. The thick bars show the OH sky emission in the upper spectrum.

ACKNOWLEDGMENTS

We are grateful to the staffs of the Koyama Astronomical Observatory for supporting various activities during the development of WINERED. We would like to acknowledge the helpful comments made by the anonymous referee. This study is financially supported by the JSPS KAKENHI (16684001) Grant-in-Aid for Young Scientists (A), JSPS KAKENHI (20340042) Grant-in-Aid for Scientific Research (B), JSPS KAKENHI (26287028) Grant-in-Aid for Scientific Research (B), JSPS KAKENHI (21840052) Grant-in-Aid for Young Scientists (Start-up), and MEXT Supported Program for the Strategic Research Foundation at Private Universities, 2008–2012 (No. S0801061) and 2014–2018 (No. S1411028).

REFERENCES

- [1] Artigau, É., Kouach, D., Donati, J. -F., Doyon, R., Delfosse, X., Baratchart, S., Lacombe, M., Moutou, C., Rabou, P., Parès, L. P., Micheau, Y., Thibault, S., Reshetov, V. A., Dubois, B., Hernandez, O., Vallée, P., Wang, S. -Y., Dolon, F., Pepe, F. A., Bouchy, F., Striebig, N., Hénault, F., Loop, D., Saddlemyer, L., Barrick, G., Vermeulen, T., Dupieux, M., Hébrard, G., Boisse, I., Martioli, E., Alencar, S. H. P., do Nascimento, J. -D., Figueira, P. “SPIRou: the near-infrared spectropolarimeter/high-precision velocimeter for the Canada-France-Hawaii telescope,” *Proc. SPIE*, 9147, 914715 (2014)
- [2] Mahadevan, S., Ramsey, L., Bender, C., Terrien, R., Wright, J. T., Halverson, S., Hearty, F., Nelson, M., Burton, A., Redman, S., Osterman, S., Diddams, S., Kasting, J., Endl, M., Deshpande, R. “The habitable-zone planet finder: a stabilized fiber-fed NIR spectrograph for the Hobby-Eberly Telescope,” *Proc. SPIE*, 8446, 84461S (2012)
- [3] Quirrenbach, A., Amado, P. J., Caballero, J. A., Mandel, H., Mundt, R., Reiners, A., Ribas, I., Sánchez Carrasco, M. A., Seifert, W., Azzaro, M., Galadí, D., Alonso-Floriano, F. J., Dreizler, S., Montes, D., Rhode, P., Stürmer, J., and the CARMENES Consortium. “CARMENES: Blue planets orbiting red dwarfs,” *Proc. EPJ Web of Conferences*, 47, 05006 (2013)
- [4] Tamura, M., Suto, H., Nishikawa, J., Kotani, T., Sato, B., Aoki, W., Usuda, T., Kurokawa, T., Kashiwagi, K., Nishiyama, S., Ikeda, Y., Hall, D., Hodapp, K., Hashimoto, J., Morino, J., Inoue, S., Mizuno, Y., Washizaki, Y., Tanaka,

- Y., Suzuki, S., Kwon, J., Suenaga, T., Oh, D., Narita, N., Kokubo, E., Hayano, Y., Izumiura, H., Kambe, E., Kudo, T., Kusakabe, N., Ikoma, M., Hori, Ya., Omiya, M., Genda, H., Fukui, A., Fujii, Y., Guyon, O., Harakawa, H., Hayashi, M., Hidai, M., Hirano, T., Kuzuhara, M., Machida, M., Matsuo, T., Nagata, T., Ohnuki, H., Ogihara, M., Oshino, S., Suzuki, R., Takami, H., Takato, N., Takahashi, Y., Tachinami, C., Terada, H.. "Infrared Doppler instrument for the Subaru Telescope (IRD)," *Proc. SPIE*, 8446, 84461T (2012)
- [5] Käufel, H. U., Siebenmorgen, R., Moorwood, A. "High Resolution Infrared Spectroscopy in Astronomy, proceedings of an ESO Workshop held at Garching, Germany, 18-21 November 2003," Springer Berlin Heidelberg, Berlin (2005)
- [6] Wright, G. S. "Spectroscopy with CGS4 on UKIRT", *Expeimental Astronomy*, 3(1) 17-24 (1994)
- [7] Greene, T. P., Tokunaga, A. T., Toomey, D. W., Carr, J. B. "CSHELL: a high spectral resolution 1-5 um cryogenic echelle spectrograph for the IRTF," *Proc. SPIE*, 1946, 313 (1993)
- [8] McLean, I. S., Becklin, E. E., Bendiksen, O., Brims, G., Canfield, J., Figer, D. F., Graham, J. R., Hare, J., Lacayanga, F., Larkin, J. E., Larson, S. B., Levenson, N., Magnone, N., Teplitz, H., Wong, W. "Design and development of NIRSPEC: a near-infrared echelle spectrograph for the Keck II telescope," *Proc. SPIE*, 3354, 566-578 (1998)
- [9] Kobayashi, N., Tokunaga, A. T., Terada, H., Goto, M., Weber, M., Potter, R., Onaka, P. M., Ching, G. K., Young, T. T., Fletcher, K., Neil, D., Robertson, L., Cook, D., Imanishi, M., Warren, D. W. "IRCS: infrared camera and spectrograph for the Subaru Telescope," *Proc. SPIE*, 4008, 1056-1066 (2000)
- [10] Käufel, H. U., Ballester, P., Biereichel, P., Delabre, B., Donaldson, R., Dorn, R., Fedrigo, E., Finger, G., Fischer, G./Franza, F., Gojak, D., Huster, G., Jung, Y/, Lizon, J. L., Mehrgan, L., Meyer, M., Moorwood, A., Pirard, J. F., Paufigue, J., Pozna, E., Siebenmorgen, R., Silber, A., Stegmeier, J., and Wegerer, S. "CRIRES: a high-resolution infrared spectrograph for ESO's VLT," *Proc. SPIE*, 5492, 1218-1227 (2004)
- [11] Käufel, H. U., Amico, P., Ballester, P., Bendek S., E. A., Bristow, P., Casali, M., Delabre, B., Dobrzycka, D., Dorn, R. J., Esteves, R., Finger, G., Gillet, G., Gojak, D., Hilker, M., Jolley, P., Jung, Y., Kerber, F., Klein, B., Lizon, J. L., Paufigue, J., Pirard, J. F., Pozna, E., Sana, H., Sanzana, L., Schmutzer, R., Seifahrt, A., Siebenmorgen, R., Smette, A., Stegmeier, J., Tacconi-Garman, L. E., Uttenthaler, S., Valenti, E., Weilenmann, U., Wolff, B. "CRIRES: commissioning and first science results," *Proc. SPIE*, 7014, 70140W (2008)
- [12] Wilson, J. C., Hearty, F., Skrutskie, M. F., Majewski, S. R., Schiavon, R., Eisenstein, D., Gunn, J., Holtzman, J., Nidever, D., Gillespie, B., Weinberg, D., Blank, B., Henderson, C., Smee, S., Barkhouser, R., Harding, A., Hope, S., Fitzgerald, G., Stolberg, T., Arns, J., Nelson, M., Brunner, S., Burton, A., Walker, E., Lam, C., Maseman, P., Barr, J., Leger, F., Carey, L., MacDonald, N., Ebelke, G., Beland, S., Horne, T., Young, E., Rieke, G., Rieke, M., O'Brien, T., Crane, J., Carr, M., Harrison, C., Stoll, R., Vernieri, M., Shetrone, M., Allende-Prieto, C., Johnson, J., Frinchaboy, P., Zasowski, G., Garcia Perez, A., Bizyaev, D., Cunha, K., Smith, V. V., Meszaros, Sz., Zhao, B., Hayden, M., Chojnowski, S. D., Andrews, B., Loomis, C., Owen, R., Klaene, M., Brinkmann, J., Stauffer, F., Long, D., Jordan, W., Holder, D., Cope, F., Naugle, T., Pfaffenberger, B., Schlegel, D., Blanton, M., Muna, D., Weaver, B., Snedden, S., Pan, K., Brewington, H., Malanushenko, E., Malanushenko, V., Simmons, A., Oravetz, D., Mahadevan, S., Halverson, S. "Performance of the Apache Point Observatory Galactic Evolution Experiment (APOGEE) high-resolution near-infrared multi-object fiber spectrograph," *Proc. SPIE*, 8446, 84460H (2012)
- [13] Wilson, J. C., Hearty, F., Skrutskie, M. F., Majewski, S., Schiavon, R., Eisenstein, D., Gunn, J., Blank, B., Henderson, C., Smee, S., Barkhouser, R., Harding, A., Fitzgerald, G., Stolberg, T., Arns, J., Nelson, M., Brunner, S., Burton, A., Walker, E., Lam, C., Maseman, P., Barr, J., Leger, F., Carey, L., MacDonald, N., Horne, T., Young, E., Rieke, G., Rieke, M., O'Brien, T., Hope, S., Krakula, J., Crane, J., Zhao, B., Carr, M., Harrison, C., Stoll, R., Vernieri, M. A., Holtzman, J., Shetrone, M., Allende-Prieto, C., Johnson, J., Frinchaboy, P., Zasowski, G., Bizyaev, D., Gillespie, B., Weinberg, D. "The Apache Point Observatory Galactic Evolution Experiment (APOGEE) high-resolution near-infrared multi-object fiber spectrograph," *Proc. SPIE*, 7735, 77351C (2012)
- [14] Oliva, E., Origlia, L., Maiolino, R., Baffa, C., Biliotti, V., Bruno, P., Falcini, G., Gavriousev, V., Ghinassi, F., Giani, E., Gonzalez, M., Leone, F., Lodi, M., Massi, F., Mochi, I., Montegriffo, P., Pedani, M., Rossetti, E., Scuderi, S., Sozzi, M., Tozzi, A. "The GIANO spectrometer: towards its first light at the TNG," *Proc. SPIE*, 8446, 84463T, 9 (2012a)
- [15] Oliva, E., Biliotti, V., Baffa, C., Giani, E., Gonzalez, M., Sozzi, M., Tozzi, A., Origlia, L. "Performances and results of the detector acquisition system of the GIANO spectrometer," *Proc. SPIE*, 8453, 84532T, 7 (2012b)
- [16] Park, C., Jaffe, D. T., Yuk, I. S., Chun, M. Y., Pak, S., Kim, K. M., Pavel, M., Lee, H., Oh, H., Jeong, U., Sim, C. K., Lee, H. I., Nguyen L., Huynh A., Strubhar, J., Gully-Santiago, M., Oh, J. S., Cha, S. M., Moon, B., Park, K., Brooks, C., Ko, K., Han, J. Y., Nah, J., Hill, P. C., Lee, S., Barnes, S., Yu, Y. S., Kaplan, K., Mace, G., Kim, H., Lee, J. J.,

- Hwang, N., Park, B. "Design and early performance of IGRINS (Immersion Grating Infrared Spectrometer)," Proc. SPIE, 9147, 91471D, 12 (2014)
- [17] Marsh, J. P., Mar, D. J., and Jaffe, D. T. "Production and evaluation of silicon immersion gratings for infrared astronomy," Applied Optics, 17, 3400-3416 (2007)
- [18] Gully-Santiago, M. A., Jaffe, D. T., Brooks, C. B., Wilson, D. W., Muller, R. E. "High performance Si immersion gratings patterned with electron beam lithography," Proc. SPIE, 9151, 91515K (2014)
- [19] Rayner, J., Bond, T., Bonnet, M., Jaffe, Dan., Muller, G., Tokunaga, A. "iSHELL: a 1-5 micron cross-dispersed R=70,000 immersion grating spectrograph for IRTF," SPIE, 8446, 84462C (2012)
- [20] Kotani, T., Tamura, M., Suto, H., Nishikawa, J., Sato, B., Aoki, W; Usuda, T; Kurokawa, T; Kashiwagi, K, Nishiyama, S, Ikeda, Y; Hall, D. B., Hodapp, K. W., Hashimoto, J., Morino, J., Okuyama, Y., Tanaka, Y., Suzuki, S., Inoue, S., Kwon, J., Suenaga, T., Oh, D., Baba, H., Narita, N., Kokubo, E., Hayano, Y., Izumiura, H., Kambe, E., Kudo, T., Kusakabe, N., Ikoma, M., Hori, Y., Omiya, M., Genda, H., Fukui, A., Fujii, Y., Guyon, O., Harakawa, H., Hayashi, M., Hidai, M., Hirano, T., Kuzuhara, M., Machida, M., Matsuo, T., Nagata, T., Onuki, H., Ogihara, M., Takami, H., Takato, N., Takahashi, Y. H., Tachinami, C., Terada, H., Kawahara, H., Yamamuro, T. "Infrared Doppler instrument (IRD) for the Subaru telescope to search for Earth-like planets around nearby M-dwarfs," Proc. SPIE, 9147, 914714, 12
- [21] Follert, R., Dorn, R. J., Oliva, E., Lizon, J. L., Hatzes, A., Piskunov, N., Reiners, A., Seemann, U., Stempels, E., Heiter, U., Marquart, T., Lockhart, M., Anglada-Escude, G., Löwinger, T., Baade, D., Grunhut, J., Bristow, P., Klein, B., Jung, Y., Ives, D. J., Kerber, F., Pozna, E., Paufigue, J., Kaeufl, H. U., Origlia, L., Valenti, E., Gojak, D., Hilker, M., Pasquini, L., Smette, A., Smoker, J. "CRIRES+: a cross-dispersed high-resolution infrared spectrograph for the ESO VLT," Proc. SPIE, 9147, 914719, 10 (2014)
- [22] Ikeda, Y., Kobayashi, N., Kondo, S., Yasui, C., Motohara, K., and Minami, A., "WINERED: a warm near-infrared high-resolution spectrograph," Proc. SPIE, 6269, 62693T (2006).
- [23] Yasui, C., Ikeda, Y., Kondo, S., Motohara, K., Minami, A., and Kobayashi, N., "Warm infrared Echelle spectrograph (WINERED): testing of optical components and performance evaluation of the optical system," Proc. SPIE, 7014, 701433, 12 (2008).
- [24] Kondo, S., Ikeda, Y., Kobayashi, N., Yasui, C., Mito, H., Fukue, K., Nakanishi, K., Kawanishi, T., Nakaoka, T., Otsubo, S., Kinoshita, M., Kitano, A., Hamano, S., Mizumoto, M., Yamamoto, R., Izumi, N., Matsunaga, N., Kawakita, H. "A Warm Near-Infrared High-Resolution Spectrograph with Very High Throughput (WINERED)," eprint arXiv:1501.03403 (2015)
- [25] in this conference
- [26] Finger, G., Dorn, R. J., Meyer, M., Mehrgan, L., Stegmeier, J., Moorwood, A. F. M. "Performance of large-format 2Kx2K MBE grown HgCdTe Hawaii-2RG arrays for low-flux applications," Proc. SPIE, 5499, 47-58 (2004)
- [27] Finger, G., Dorn, R. J., Eschbaumer, S., Hall, D. N. B., Mehrgan, L., Meyer, M., Stegmeier, J. "Performance evaluation, readout modes, and calibration techniques of HgCdTe Hawaii-2RG mosaic arrays," Proc. SPIE, 7021, 70210P, 13 (2008)
- [28] Hamano, S. et al. in preparation
- [29] Joyce, R. R., Hinkle, K. H., Meyer, M. R., Skrutskie, M. F. "Infrared astronomical spectroscopy with a noncryogenic spectrograph," Proc. SPIE, 3354, 741-749
- [30] Sheinis, A. I., Wolf, M. J., Bershady, M. A., Buckley, D. A. H., Nordsieck, K. H., Williams, Ted B. "The NIR upgrade to the SALT Robert Stobie Spectrograph," Proc. SPIE, 6269, 62694T (2006)
- [31] Amado, P. J., Lenzen, R., Cardenas, M. C., Sánchez-Blanco, E., Becerril, S., Sánchez-Carrasco, M. A., Seifert, W., Quirrenbach, A., Ribas, I., Reiners, A., Mandel, H., Caballero, J. A. "CARMENES. V: non-cryogenic solutions for YJH-band NIR instruments," Proc. SPIE, 8450, 84501U, 13
- [32] Clough, S.A., M.J. Iacono, and J.-L. Moncet, "Line-by-line calculation of atmospheric fluxes and cooling rates: Application to water vapor," J. Geophys. Res., 97, 15761-15785, (1992)
- [33] Clough, S. A., M. W. Shephard, E. J. Mlawer, J. S. Delamere, M. J. Iacono, K. Cady-Pereira, S. Boukabara, and P. D. Brown, "Atmospheric radiative transfer modeling: a summary of the AER codes," Short Communication, J. Quant. Spectrosc. Radiat. Transfer, 91, 233-244, (2005)
- [34] Sameshima, H. et al. in preparation
- [35] Groh, J. H., Damineli, A.s, and Jablonski, F., "Spectral atlas of massive stars around He I 10830 Å," Astronomy and Astrophysics, Volume 465, Issue 3, pp.993-1002 (2007)

- [36] Hamano, S., Kobayashi, N., Kondo, S., Ikeda, Y., Nakanishi, K., Yasui, C., Mizumoto, M., Matsunaga, N., Fukue, K., Mito, H., Yamamoto, R., Izumi, N., Nakaoka, T., Kawanishi, T., Kitano, A., Otsubo, S., Kinoshita, M., Kobayashi, H., and Kawakita, H., "Near-infrared Diffuse Interstellar Bands in 0.91-1.32 μm ," *The Astrophysical Journal*, Volume 800, Issue 2, article id. 137, 17 pp. (2015)
- [37] Hamano, S., Kobayashi, N., Kondo, S., Sameshima, H., Nakanishi, K., Ikeda, Y., Yasui, C., Mizumoto, M., Matsunaga, N., Fukue, K., Yamamoto, R., Izumi, N., Mito, H., Nakaoka, T., Kawanishi, T., Kitano, A., Otsubo, S., Kinoshita, M., and Kawakita, H. "Near Infrared Diffuse Interstellar Bands Toward the Cygnus OB2 Association," *The Astrophysical Journal*, 821, Issue 1, article id. 42, 12 pp. (2016)
- [38] Hamano, S., Otsubo, S., Ikeda, Y., et al. in preparation
- [39] Kawakita, H., Shinnaka, Y., Ogawa, S., Kobayashi, H., Kondo, S., Nakanishi, K., Kawanishi, T., Nakaoka, T., Otsubo, S., Kinoshita, M., Ikeda, Y., Yamamoto, R., Izumi, N., Fukue, K., Hamano, S., Yasui, C., Mito, H., Matsunaga, N., Kobayashi, N. "High Resolution Near-Infrared Spectroscopy of Comet C/2013 R1 (Lovejoy) using WINERED at Koyama Astronomical Observatory," *American Astronomical Society, DPS meeting #46, id.209.16* (2014)